Tanzania Journal of Science 45(3): 450-462, 2019 ISSN 0856-1761, e-ISSN 2507-7961

Quantitative Assessment of Resistivity Anisotropy in Evaluation of Laminated Shaly Sand Hydrocarbon Reservoirs–A Case Study in the Barents Sea, Norway

Ernest S Mulaya
Department of Geology, University of Dar es Salaam, P. O. Box 35052 Dar es Salaam, Tanzania
E-mail address: mulaya1985@yahoo.com

Abstract

Resistivity anisotropy in shaly sand lamination sequences affects the hydrocarbon evaluation in multiple dimensions of petrophysical logs. Currently, vertical resistivity (Rv) and horizontal resistivity (Rh) from 3D triaxial induction measurements can be applied simultaneously to resolve these petrophysical impacts. In this paper, an extensive analysis is offered with a focus on the hydrocarbon evaluation based on advanced petrophysical logs from a well. A critical analysis is done on the three comparable cases including clean formation as a base case, shaly sand case and laminated shaly sand case towards resolving resistivity anisotropy in a typical shaly sand laminated reservoir. The analysis results into potential pay zones of 38.0 m thick of gas and 76 m thick for oil. Furthermore, the results provide an increase in hydrocarbon pore fraction (HCPF) per depth up to 30% in zones with Rv/Rh ratio greater than or equal to 3 compared to conventional evaluation. The study concludes that in a lithology of shale sand laminated sequences, the feasible evaluation technique of hydrocarbon should involve the combination of derived hydrocarbon bearing sand lamina resistivity (Rsand) from horizontal (Rh) and vertical resistivity (Rv) of triaxial induction measurement, refined sand porosity from Thomas Stieber model and associated net to gross using the shaly sand models.

Keywords: Resistivity anisotropy, laminated shaly sand, triaxial induction measurements, density magnetic resonance porosity, hydrocarbon evaluation

Introduction

Laminated shaly sands, as the name implies, refers to alternating thin layers of sands and shale leading to differences in their vertical and horizontal electrical properties (resistivity anisotropy) (Clavier et al. 1984, Worthington 1985, Herrick and Kennedy 1996, Ellis and Singer 2008). The laminated shaly sand formations are very significant reservoirs for oil and gas despite exhibiting 'low resistivity pay' (Worthington 2000, Clavaud et al. 2005). The increased content of shale decrease the effective reservoir capacity (Anderson et al. 1995, Gluyas and Swarbrick 2013). At the same time, the electrical properties, i.e., conductivity of shales reduce the formation resistivity, hence must be corrected for the evaluations and identification of net pay and reliable assessment of hydrocarbon saturation.

Induction resistivity is based on the alternative currents in the transmitter coils which set up an alternative magnetic field in the conductive magnetic field (Ellis and Singer 2008). The effects of resistivity anisotropy on the induction resistivity measurement have been known since the 1950's (Kunz and Gianzero 1958, Moran and Gianzero 1979, Anderson et al. 2008). The problems associated with resistivity anisotropy become acute in a thinly laminated shaly sand formation whose beds are thinner than the vertical resolution of the conventional resistivity and porosity measurement tools (Anderson and Gianzero 1982, Berg et al. 1996, Klein and Martin 1997, Mollison et al.

1999, Schoen et al. 1999, Anderson et al. 2008). The hydrocarbon saturation interpreted from the conventional resistivity measurements in these formation gives the cumulative or weighted average of the individual layers response of both shale and sand lamina consequently lowering the hydrocarbon estimation (Anderson et al. 1997). This is because the computations involved are petrophysically dominated by high conductive shale/clay effects which obscure the presence of more resistive hydrocarbon bearing sands (Boyd et al. 1995, Fanini et al. 2001, Clavaud et al. 2005).

Therefore, this paper reports on three comparable cases including clean formation case, shaly sand case and laminated shaly sand case from which the impact of resistivity anisotropy in laminated shaly sand reservoirs can further be refined and resolved both mathematically and petrophysically. This is based on the vertical resistivity (Rv) and horizontal resistivity (Rh) from 3D triaxial induction measurement towards maximizing hydrocarbon evaluation.

Materials and Methods

Study area

This study used data from the exploration well 7220/8-1 located in the Southwestern Barents Sea, Norway (coordinates: 72° 29' 28.92" N, 20° 20' 2.25" E) (NPD 2019) (Figure 1).

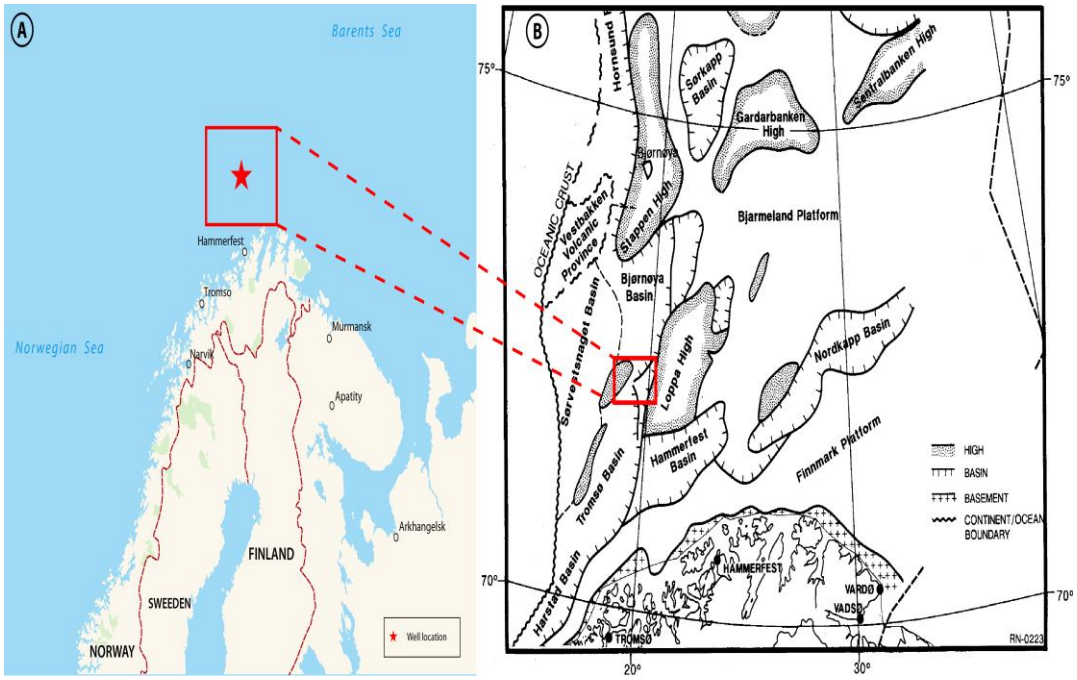

Figure 1: Geographical and geological location of the study area: (A) Geographical location of well 7220/8-1 at the Western Barents Sea (star in a square). (B) Tectonic framework of the Barents Sea region, the well 7220/8-1 drilled just west of the Polheim Sub-platform and Loppa High (Gabrielsen et al. 1990, Lřseth et al. 2013).

Data availability, software loading and quality control

The input well logs data in Digital Log Interchange Standards (DLIS format) acquired by Schlumberger from a well in the Barents Sea were interpreted using Techlog™ software (Techlog64 2013.4.0) licensed by Schlumberger Company. Data

quality were checked for their reliability and addressed leading to the initial choice of the appropriate data sets, parameters and feasible methodology. The well logs data used in this study were environmentally corrected during logging hence no further corrections were made.

Triaxial induction (Rv/Rh) values

Vertical resistivity (Rv) and horizontal resistivity (Rh) values from 3D triaxial induction tool inferring electrical anisotropy were used to derive the true formation resistivity (Fanini et al. 2001, Wang et al. 2006, Anderson et al. 2008). The triaxial measured value is based on the fact that when the measurement is made parallel to the sand-shale layers, the results are similar to measuring resistance in parallel while when the measurement is made across the lamination stacks the measured value is similar to measuring resistance in series (Shray and Borbas 2001). The large difference between vertical resistivity (Rv) and horizontal resistivity (Rh) is an indication of resistivity anisotropy (Shray and Borbas, 2001, Clavaud et al. 2005, Anderson et al. 2008). For a laminated sand-shale sequence, the portion of the reservoir that is of interest is the one with hydrocarbon bearing sand package whose resistivity (R_{snd}), volume of shale (V_{sh}) and volume of sand (V_{snd}) were derived from the methodologies illustrated by Shray and Borbas (2001), Clavaud et al. (2005) and Anderson et al. (2008) as shown in the following section.

Resolving sand resistivity involves initial inputs of horizontal resistivity (Rh) and vertical resistivity (Rv) derived from triaxial induction tool in Equations (1) and (2) with additional argument in Equation (3) below;

$$R_V = V_{sh} * R_{sh} + V_{snd} * R_{snd} \qquad (1)$$

$$\frac{1}{Rh} = \frac{V_{sh}}{R_{sh}} + \frac{V_{snd}}{R_{snd}} \qquad (2)$$

Where:

$$1 = V_{sh} + V_{snd} \qquad (3)$$

The solution for the two Equations (1) and (2) as suggested by Shray and Borbas (2001), Clavaud et al. (2005), Wang et al. (2006) and Anderson et al. (2008) can be mathematically simplified in Equations (4) and (5) below;

$$R_{snd} = R_h\left(\frac{R_v - R_{sh}}{R_h - R_{sh}}\right) \qquad (4)$$

$$V_{snd} = \left(\frac{R_v - R_{sh}}{R_{snd} - R_{sh}}\right) \qquad (5)$$

In mathematical sense, the following boundary conditions should be applied to obtain a continuous computation versus depth of the formation fluid volumes to avoid blow ups according to Shray and Borbas (2001);

i. The computed value of R_h should not be equal to R_{sh}.
ii. The computed value of R_{snd} should not be equal to our picked R_{sh}.

Resistivity of shale (R_{sh}) and sand (R_{snd})

The resistivity of shale is an integral component of shaly sand saturation models. The value of shale resistivity (R_{sh}) of 3 ohm m was estimated from the adjacent pure shale zone between 1249.7 and 1276.0 m, the zone assumed to be 100% shale. This value was used to solve for R_{snd} and volume of sand (V_{snd}) in Equations (4) and (5). On the other hand, the resistivity of sand (R_{snd}) derived from triaxial values (Rv/Rh) was calculated using Equation (4) in Techlog^{TM} software. The results were simultaneously used to calculate sand fraction (V_{snd}) in Equation (5).

Resistivity of water (R_w)

R_w is an integral part and interpretation parameter used in calculation of all saturations (water and/or hydrocarbon) from the resistivity logs. Therefore, Rw was computed based on resistivity ratio method under which the formation was partitioned into flushed and noninvaded zone having the same formation factor (F) but each

containing water of different resistivity measured from petrophysical logs using Equation 6 (Archie 1942 and Peveraro 1992).

$$\frac{R_w}{R_t} = \frac{R_{mf}}{R_{xo}} \qquad (6)$$

The Equation 6 above was applied in a water zone where both water saturation in uninvaded formation (Sw) and in fully flushed zone (Sxo) are 100% with their respective resistivity denoted as R_t and R_{xo}. The R_{xo}/R_t ratio was calculated over the interval evidently most clean and fully invaded water sand. Using the resistivity of mud filtrate (R_{mf}) as reported on log header, the R_w was calculated. At a depth interval of 1414.5 - 1420.0 m an average R_t, average R_{xo} and R_{mf} at maximum recorded temperature (extracted from logs header) were 0.6 ohm m, 1.5 ohm m and 0.132 ohm m, respectively. Hence a value of 0.053 ohm m was used as R_w input for computations throughout this study (Equation 6a).

$$R_w = R_{mf} * \frac{R_t}{R_{xo}} = 0.132 * 0.6/1.5 = 0.053 \text{ ohm m} \qquad (6a)$$

Density Magnetic Resonance Porosity (DMRP)

The porosity model used in this study was determined by Density Magnetic Resonance Porosity (DMRP) method. The method gives a gas refined total cross porosity combination of the density log derived porosity (DPHI) and Total Combinable Magnetic Resonance (TCMR) measurement (Freedman et al. 1998). The Equations 7 - 12 for this model are based on new gas equations derived and applicable to reservoirs with mainly gas and also gas condensate or light oil near the wellbore to provide new petrophysical equations for gas-corrected total formation porosity (Freedman et al. 1997, 1998).

Based on Freedman et al. (1998), the bulk density is given as;

$$\rho_b = \rho_{ma}(1-\varphi) + \rho_f\varphi\left(1 - S_{g,xo}\right) + \rho_g\varphi S_{g,xo} \qquad (7)$$

While simultaneously the TCMR porosity is given as;

$$TCMR = \varphi S_{g,xo}(HI)_g P_g + \varphi\left(1 - S_{g,xo}\right)(HI)_f \qquad (8)$$

Where; ρ_b= measured formation bulk density (g/cm^3); ρ_{ma} = formation matrix density (g/cm^3); ρ_f = density of liquid phase in the flushed zone at reservoir conditions (g/cm^3); ρ_g= density of gas at reservoir conditions (g/cm^3); φ = total formation porosity; $(HI)_f$ = hydrogen index of liquid phase in the flushed zone at reservoir conditions; $(HI)_g$ = hydrogen index of gas at reservoir conditions, $S_{g,xo}$ = flushed-zone gas saturation.

$$P_g = 1 - \exp\left(-\frac{W}{T_{1,g}}\right) \qquad (9)$$

Where; W = wait time for CPMG pulse sequence (s); $T_{1,g}$ = gas longitudinal relaxation time at reservoir conditions (s).

In solving the two Equations (7) and (8) simultaneously, the new parameter (10) below is introduced;

$$\lambda = \frac{\rho_f - \rho_g}{\rho_{ma} - \rho_f} \qquad (10)$$

The parameter λ is proportional to the density difference between the gas and the liquid phases and is responsible for the gas effect on the density log porosity (Freedman et al. 1998).

From the density derived porosity in Equation 11 below, then according to Freedman (1997) the total formation density magnetic resonance porosity (DMRP) is given in Equation 12.

$$DPHI = \frac{\rho_b - \rho_{ma}}{\rho_f - \rho_{ma}} \qquad (11)$$

$$DMRP(\varphi) = \frac{DPHI * \left(1 - \frac{(HI)_g * P_g}{(HI)_f}\right) + \frac{\lambda * TCMR}{(HI)_f}}{\left(1 - \frac{(HI)_g * P_g}{(HI)_f}\right) + \lambda} \qquad (12)$$

Assumptions of the methodology;

i. The wait time is sufficiently long to polarise the liquid phase hence

polarization function of the liquid (P_f = 1) (Freedman et al. 1998).

ii. The following input parameters and uncertainties were derived from the literature (Freedman et al. 1998) (Table 1).

Table 1: Input parameters used in the methodology for Equations 7-12 based on Freedman et al. (1998)

ρ_{ma}	ρ_f	ρ_g	$T_{1,g}$	$(HI)_g$	$(HI)_f$	W
2.65	1.0	0.26	6.0	0.47	1.0	6.0

These uncertainties and input parameters reflect our lack of detailed knowledge of a particular parameters and uncertainties in measured log responses. The calculation for all these parameters were computed in Techlog^{TM} software for use in workflow with other petrophysical parameters.

Hydrocarbon evaluation

The hydrocarbon saturations were evaluated as a compliment of water saturation (1-S_w). In this study, the water saturation (S_w) models considered included Archie, modified Simandoux and Poupon Leveaux (Indonesia) models from which the impacts of resistivity anisotropy were analyzed (Archie 1942, 1950, 1952, Bardon and Pied 1969, Poupon et al. 1970, Leveaux and Poupon 1971). These models were chosen because they cover both shaly and non shaly settings during hydrocarbon evaluation.

Archie model

Archie's saturation model (Equation 13) was used as a base case in this study assuming non shaliness scenarios; no electrical conductivity in the rock framework; only electrolyte brine water is present as per Archie (1942, 1950, 1952).

$$S_W = \left[\frac{a*R_w}{\varphi^m * R_t}\right]^{\frac{1}{n}} \qquad (13)$$

Where; Sw = water saturation (Archie) [%], a = lithology factor [unitless], Rw = water resistivity [ohm-m], φ= total porosity [%], m = cementation factor [unitless], Rt = bulk resistivity [ohm-m], n = saturation exponent (unitless), a = 1, n = m = 2 based on the provided core report.

Shaly sand saturation models

Two shaly sand saturation models both taking on board the volume of shale/clay (Vclay) were considered in evaluation of hydrocarbon saturation using modified Simandoux and Poupon Leveaux/Indonesia models as illustrated by Bardon and Pied (1969), Poupon et al. (1970) and Leveaux and Poupon (1971).

Results and Discussion

Formation porosity

The Density Magnetic Resonance Porosity (DMRP) derived from the combination of the log density (DPHI) and total nuclear magnetic resonance porosity (TCMR) comparatively showed the best match with the core porosity ranging between 25 and 28%. This match is because the DMRP considers the combined effects of shaliness and gas that proves its appropriateness in both shale and hydrocarbon zones of the studied well. This is in agreement with the results by La Vigne et al. (1994) and Freedman et al. (1998).

Resistivity anisotropic zones

The anisotropic zones were identified by analysing the difference in vertical resistivity (Rv) and horizontal resistivity (Rh) of triaxial induction measurements (Figure 2, track 3). The degree of resistivity anisotropy in different zones is indicated by the ratio between Rv and Rh greater than 3 (Rv/Rh > 3) complemented by Nuclear Magnetic Resonance (NMR) relaxation time (T2) distribution curve (Figure 2, tracks 4 & 5). The bimodal relaxation of T2 distribution bisected by the solid vertical cut off line at 33 milliseconds (msec) corresponds to both clay bound water and free fluid in laminated shaly sand zones, notably when the Rv/Rh ratio is greater than 3 (Figure 2, track 4). These zones were clearly identified in intervals from 1278.0 to 1292.0 m, 1302.0 to

1312.0 m and 1354.0 to 1390.0 m indicating the presence of high anisotropy attributable to thin laminated shaly sand sequences less than 10 mm (red boxes in Figure 2). The ratio of vertical resistivity (Rv) and horizontal resistivity (Rh) from the triaxial induction measurement when greater than 3 (Rv/Rh > 3) also confirms anisotropic zones different from the values greater than 5 as reported by Klein (1996), Klein and Martin (1997), Kennedy and Herrick (2004). The differences in Rv/Rh ratios can be attributable to diversity of volume of clay in the reservoir. In addition, the observed lithology and core description report for this well also documented shaly sand laminations in the same intervals.

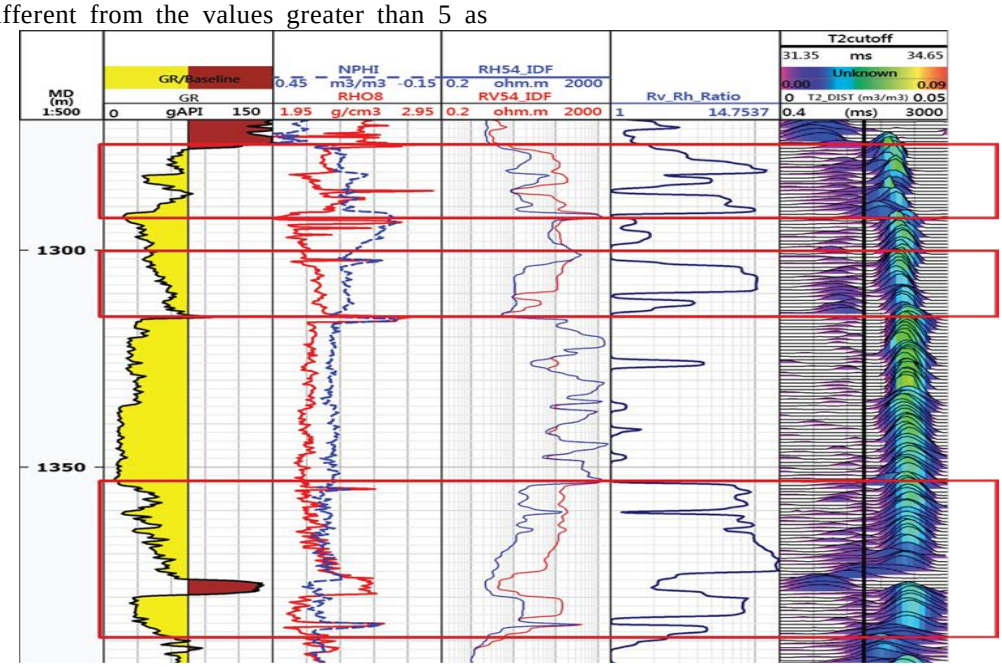

Figure 2: The anisotropic zones illustrated in red boxes for the intervals between 1278.0 - 1292.0 m, 1302.0 - 1315.0 m and 1354.0 - 1390.0 m corresponding to bimodal relaxation of T2 distribution (track 5). The resistivity anisotropy gives Rv and Rh ratios greater than 3 (Rv/Rh > 3) (track 4).

Fluid bearing zones

Three fluid types (gas, oil and water) were identified based on log interpretations and formation pressure testing data. Generally, fluid zones were identified by mainly large change in formation resistivity with no significant change in porosity (DMRP) and lithology. The gas bearing zones were identified in the depth zones between 1276.8 and 1315 m and oil zone between 1317.0 and 1399.0 m, and the water zone below 1400.0 m (Figure 3). Specifically, the hydrocarbon bearing zones are characterized by large negative separation between neutron and density log curves (excavation effects typical for gas) complemented by extremely high resistivity (500 - 2000 ohm m), low gamma ray response (15 - 40 API) and high porosity (25%). On the other hand, the water bearing zone exhibits relatively lower resistivity (0.01 - 0.5 ohm m) corresponding to high porosity (25%) (Figure 3).

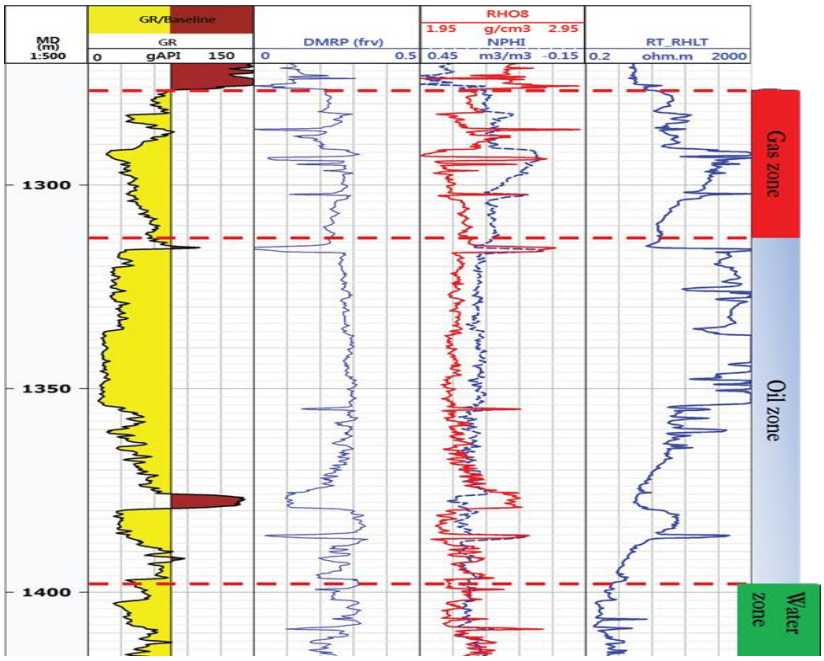

Figure 3: Fluid zones as indicated by log data; gas zone interval from 1276.8 to 1315 m, oil zone interval from 1317.0 to 1399.0 m and the water zone below 1400.0 m.

Reservoir fluid types

The presence of different reservoir bearing fluids such as; gas, oil and water in the well were also confirmed by the pressure gradients obtained from formation pressure test data plotted against the true vertical depths (TVD) obtained from Modular Formation Dynamics Tester (MDT). The results showed that this well encountered a gas 'pay interval' of approximately 37.0 m thick below the thick shale, which could possibly be the cap rock used to recharge the present oil and gas reservoir. Based on the changes on the regression line or fluid gradient, the gas oil contact (GOC) was interpreted at 1315.0 m and the oil water contact (OWC) at 1399.0 m (Figure 4). These intervals and contacts are in agreement with previous results published by Norwegian Petroleum Directorate (NPD 2019).

Net pay zones

The net pay calculated purposely to eliminate nonproductive rock intervals in this wellbore resulted into depths ranging from 1276.8 to 1395.0 m. The net pay provided depths for calculating the hydrocarbon pore fraction (HCPF) and hydrocarbon pore column (HCPC), both implying the amount of hydrocarbon bearing space. The cut offs applied for both Case 1 and Case 2 described in the following sections include porosity greater than 10% (Phi > 0.10), water saturation less than 65% (0 < Sw < 0.65 v/v) and clay content (Vclay) less than 40% against which the resistivity anisotropic impacts were analyzed (Galley 2016). The net to gross ratio from Thomas Stieber model was applied to Case 3 in agreement with those of Anderson et al. (2008).

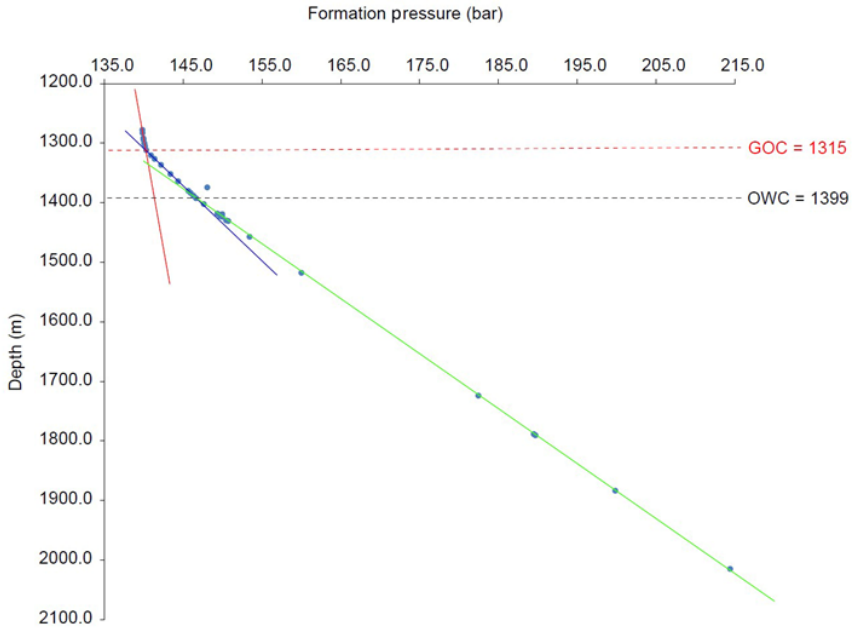

Figure 4: The MDT gradient plot showing the gas gradient (red line), oil gradient (blue line) and water gradient (green line) defining the gas oil contact (GOC at 1315 m) and oil water contact (OWC at 1399 m).

Hydrocarbon saturation and volumes

The hydrocarbon saturation (S_{hc}) as a complement of water saturation (1 – Sw) was calculated within considerable net pay, hydrocarbon pore fraction (HCPF), hydrocarbon pore column (HCPC) and the volume of hydrocarbon in place. The hydrocarbon volume and column were computed based on HCPF and HCPC, respectively in zones specified by cut offs by considering their productive pay thickness (ΔZ) and net to gross (Equations 14 and 15).

$$\mathrm{HCPF} = \varphi * (1 - \mathrm{Sw}) \quad (14)$$

$$\mathrm{HCPC} = \sum \varphi * (1 - \mathrm{Sw}) * \Delta Z * \mathrm{Net/Gross} \quad (15)$$

The incremental pay thickness was constant (ΔZ = 0.076 m) based on different logs per depth (logging interval) for the given data of the well 7220/8-1. The results for three cases are given below.

Case 1: Clean formation assumption

This case, ideally clean sand, was used as a base case applying Archie model along which the other two cases were compared. This resulted into less water saturation between 1 and 5% corresponding to high resistivity ranging between 1000 and 2000 ohm m and high porosity (DMRP) of 28% in the zone ranging from 1317.0 to 1354.0 m (Nordmela Formation). These petrophysical parameters are typical responses from the zones fully occupied by hydrocarbon fluids implying huge hydrocarbon saturation (1 - Sw) between 95 and 99%. The interval from 1375.0 to 1380.0 m exhibits typical shale zone with extremely high water saturation (100%) due to high clay bound fluids and low resistivity of 3.0 ohm m. In the base case, the potential pay zones ranged from 1276.8 to 1315.0 m and 1316.5 to 1393.8 m for gas zone and oil zone, respectively, whereby HCPFs per depth were between 0.10 and 0.37 v/v. The summation of hydrocarbon

pore column accounts to 7.19 m of gas and 15.54 m for oil (Table 2).

Table 2: Summary of hydrocarbon pore column (HCPC) for both gas and oil bearing zones summed for the clean formation assumption (base case) using Archie's equation

Fluid type	Depth range (m)	Thickness (m)	HCPC (m)
Gas bearing	1276.8–1315	38.2	7.19
Oil bearing	1316.5–1393.8	77.3	15.54
	Total (m)	115.5	22.73

Case 2: Shaly sand assumption

Different from Case 1 above, Case 2 considered the shale component/ shaliness effects in the reservoir using the volume of shale/clay (Vclay) as one of the input in two shaly sand equations namely modified Simandoux equation and Poupon Leveaux/Indonesia equation. Water saturation computed from both shaly sand models showed too small differences of 2 - 4% in the zone between 1276.8 and 1354.0 m which is petrophysically negligible. This is due to the fact that this zone is relatively cleaner (less clay amount), therefore all the saturation models converge closer to Archie's assumptions specifically in the respective zone (Archie, 1942, 1950, 1952). The zone between 1354.0 and 1400.0 m is characterized by laminated shale sand where the Indonesian model resulted into comparatively lower water saturation by 2–4% than modified Simandoux model. The negligible minor difference between the two models in relatively cleaner zone is merely due to quadratic nature of the later model (Bardon and Pied 1969, Leveaux and Poupon 1971).

On the other hand, the modified Simandoux model gave out hydrocarbon pore column of 7.57 m for gas leg and 16.5 m for oil leg in the hydrocarbon zones ranging from 1276.8 to 1315.0 m and 1316.5 to 1395.2 m, respectively making a total of 24.07 m HCPC (Table 3), while the hydrocarbon pore fractions per depth ranged between 0.10 and 0.37 v/v. In this case, the HCPC increases significantly by 6% from 22.73 m to 24.07 m for Case 1 and Case 2, respectively due to the fact that latter considers the shaliness/clay volumes reducing effects in computation while the former considers the formation as bulk resolvable zone. These operation approaches compromise the cut off elements during evaluation, i.e., porosity, permeability and resistivity (Ellis and Singer 2008).

Table 3: Summary of HCPC for both gas and oil bearing zones summed for the shaly sand case based on modified Simandoux model

Fluid type	Depth range (m)	Thickness (m)	HCPC (m)
Gas bearing	1276.8–1315	38.2	7.57
Oil bearing	1316.5–1393.8	78.7	16.5
	Total (m)	116.9	24.07

Case 3: Laminated Shaly Sand (LSS) assumption

Under this case, the evaluation was approached as anisotropy composed of both laminated sand-shale sequences including dispersed shale component also as per Thomas Stieber model to account for resistivity anisotropy (Thomas and Stieber 1975). Using modified Simandoux water saturation from the laminated shaly sand resulted into the lowest values between 2 and 5% specifically in laminated intervals between 1354.0 and 1375.0 m implying much hydrocarbon saturation than the other two cases.

Huge differences in water saturation between different saturation models (Simandoux being lower) were noticeable in the laminated zones characterized by high Rv/Rh ratio greater than 3 in the interval between 1354.0 and 1375.0 m. The zone where

the formation is relatively cleaner from 1317.0 to 1354.0 m is characterized by very low clay volumes (0.20 v/v) indicating no evidence of anisotropy and also revealed by low Rv/Rh ratio < 3. The zone between 1317.0 and 1354.0 m which is relatively cleaner and thicker formation, all the resistivity measurements also become close and similar in all three cases indicating that the clay effects are negligible and therefore the shaly sand equations reduce to clean Archie equation. That is why in this zone, water saturation for both Case 1 and Case 2 resulted into a slight difference compared to Case 3. This implies that the conventional resistivity measurement is more accurate than the derived sand resistivity (Rsand) in the clean zone/formation without resistivity anisotropy as per assumptions made by Archie (1942, 1950, 1952) and as per response of multiarray induction measurement analyzed by Anderson et al. (1999).

The hydrocarbon pore column of gas leg and oil leg were summed to 6.43 m and 14.45 m, respectively making a total of 20.88 m HCPC (Table 4). The HCPC was lower by 8% in the intervals of resistivity anisotropy corresponding to higher Rv/Rh ratio > 3 (Table 4). This is due to significant decrease of net to gross ratio caused by shaly sand lamination sequences thus causing a reducing effects to HCPC (Equation 15).

Table 4: Summary of HCPC for both gas and oil bearing zones summed for the laminated shaly sand (LSS) case based on modified Simandoux equation

Fluid type	Depth range (m)	Thickness (m)	HCPC (m)
Gas bearing	1276.8–1315	38.2	6.43
Oil bearing	1316.5–1393.8	78.8	14.45
	Total (m)	117	20.88

Hydrocarbon increment

The laminated shaly sand (LSS) in Case 3 resulted into the highest hydrocarbon pore fraction (HCPF) per depths particularly in the whole gas interval between 1276.8 and 1315.0 m. Much of the hydrocarbon enhancements account up to 30% increase of hydrocarbon saturation in highly anisotropic/laminated zones at depth interval between 1302 and 1310 m (Figure 5, track 5 in red box). The significant hydrocarbon increment in Case 3 is due to resolving power of anisotropy in the reservoir based on triaxial induction measurements and density magnetic resonance porosity. Furthermore, the hydrocarbon increase in terms of HCPF up to 30% shows the power of laminated shaly sand (LSS) approach in enhancing the hydrocarbon saturation and counter resistivity anisotropy. This significant hydrocarbon increment would otherwise be underestimated up to 60% if convention petrophysical measurements were applied as described by Anderson et al. (2008).

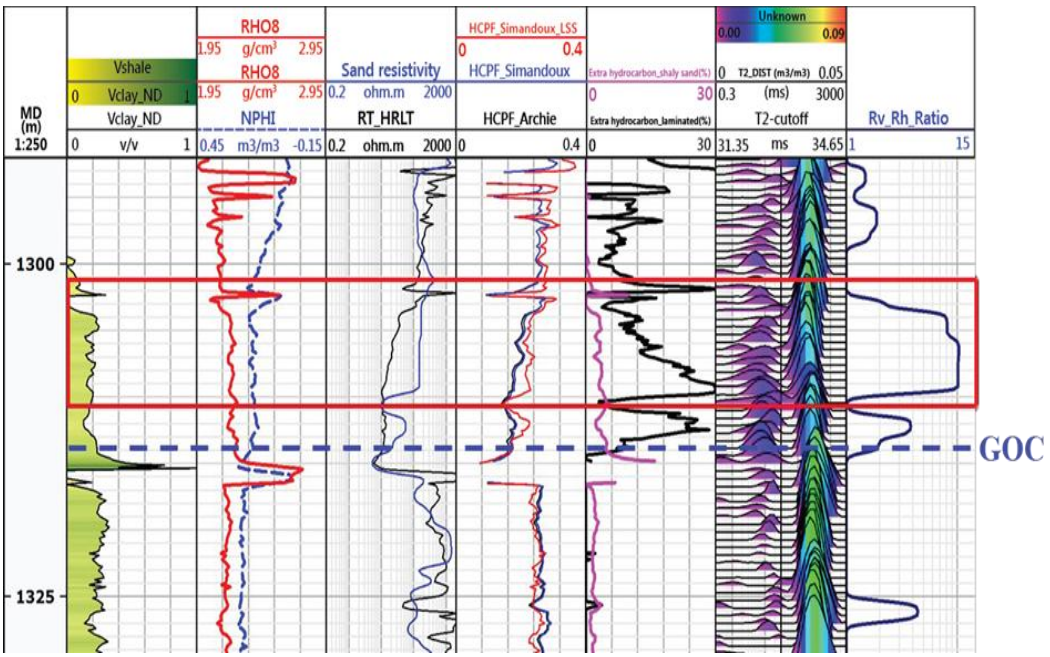

Figure 5: Increase in HCPF in gas and highly anisotropy zone (red box) up to 30% of HCPF in laminated shaly sand (black curve, track 5) and less increment in shaly sand (pink curve, track 5).

Conclusions

The degree of anisotropy was indicated by resistivity ratio (Rv/Rh) when is equal to or greater than 3. This is attributed to thin laminated sand shale sequences clearly interpreted in the intervals from 1278.0 to 1292.0 m, 1302.0 to 1312.0 m and 1354.0 to 1390.0 m. This well is comprised with approximately gas column of about 38.0 m thick, oil column of about 76 m thick and water below the oil zone. The incremental increase in hydrocarbon pore fraction (HCPF) per depth up to 30% in laminated shaly sand (Case 3) compared to Case 1 and Case 2 implying that significant hydrocarbon can be quantified in a thinner column/thickness which would otherwise be left out. Therefore, in a lithology setting of shaly sand laminated sequences, the feasible and reliable evaluation technique of the hydrocarbon potential should preferably involve the combination of derived hydrocarbon bearing sand lamina resistivity (Rsand) from horizontal (Rh) and vertical resistivity (Rv) of triaxial induction measurements and refined sand porosity from Thomas Stieber model and associated net to gross ratio using the shaly sand equations to give the reasonable results pertaining to hydrocarbon volumes.

Acknowledgements

This work was funded by NORAD/Statoil scholarship, the results of which are part of the author's Master's degree thesis of 2015, offered by the Norwegian University of Science and Technology (NTNU). The author thanks Professor Erik Skogen from Norwegian University of Science and Technology and Dr. Isaac Marobhe from University of Dar es Salaam for their guidance towards achievement of this study.

References

Anderson B and Gianzero S 1982 A new look at skin effect. *Log Anal.* 23(01).

Anderson BI, Barber TD and Luling MG 1995 The response of induction tools to dipping, anisotropic formations. In *SPWLA 36th Annual Logging Symposium*, Paper D.

Anderson B, Druskin V, Habashy T, Lee P, Lüling M, Barber T, Grove G, Lovell J, Rosthal R, Tabanou J and Kennedy D 1997 New dimensions in modelling resistivity. *Oil. Rev*. 9(1): 40-56.

Anderson B, Barber T, Davydycheva S, Vladimir D, Dussan E, Knizhnerman L and Lee P 1999 The response of multiarray induction tools in highly dipping formations with invasion and in arbitrary 3D geometries. *Log Anal*. 40(05): 327-344.

Anderson B, Barber T, Bastia R, Clavaud J, Coffin B, Das M, Hayden R, Klimentos T, Minh CC and Williams S 2008 Triaxial induction–A new angle for an old measurement. *Schlumberger Oilfield Review*. Summer edition, 84 pp.

Archie GE 1942 The electrical resistivity log as an aid in determining some reservoir characteristics. *Trans. AIME* 146(01): 54-62.

Archie GE 1950 Introduction to petrophysics of reservoir rocks. *AAPG Bul.* 34(5): 943-961.

Archie GE 1952 Classification of carbonate reservoir rocks and petrophysical considerations. *AAPG Bulletin* 36(2): 278-298.

Bardon C and Pied B 1969 Formation water saturation in shaly sands. In *SPWLA 10th Annual Logging Symposium*, Paper z.

Berg FG, Looyestijn WJ and Sandor RK 1996 Sandwich: Log evaluation in laminated shaly sands. In *SPWLA 37th Annual Logging Symposium*, Paper BB.

Boyd A, Darling H, Tabanou J, Davis B, Lyon B, Flaum C, Klein J, Sneider RM and Singer MJ 1995 The lowdown on low-resistivity pay. *Oil. Rev.* 7(3): 4-18.

Clavaud JB, Nelson R and Guru UK 2005 Field example of enhanced hydrocarbon estimation in thinly laminated formation with a triaxial array induction tool: A laminated sand-shale analysis with anisotropic shale. In *SPWLA 46th Annual Logging Symposium*, Paper W.

Clavier C, Coates G and Dumanoir J 1984 Theoretical and experimental bases for the dual-water model for interpretation of shaly sands. *Soc. Petrol. Engin. J'* 24(02): 153-168.

Ellis DV and Singer JM 2008 Well logging for earth scientists. 2nd ed, Springer, Dordrecht, Netherlands.

Fanini ON, Kriegshäuser BF, Mollison RA, Schön JH and Yu L 2001 Enhanced, low-resistivity pay, reservoir exploration and delineation with the latest multicomponent induction technology integrated with NMR, nuclear, and borehole image measurements. In *Offshore Technology Conference*, Paper 69447.

Freedman R, Boyd A, Gubelin G, McKeon D, Morriss CE and Flaum C 1997 Measurement of total NMR porosity adds new value to NMR logging. In *SPWLA 38th Annual Logging Symposium*, Paper OO.

Freedman R, Minh CC, Gubelin G, Freeman JJ, McGinness T, Terry B and Rawlence D 1998 Combining NMR and density logs for petrophysical analysis in gas-bearing formations. In *SPWLA 39th Annual Logging Symposium*.

Gabrielsen RH, Færseth RB, Jensen LN, Kalheim JE and Riis F 1990 Structural elements of the Norwegian continental shelf, Part I: The Barents Sea. *Bull*. 6: 33 pp.

Galley SV 2016 Pay Cutoff definition based on dynamic reservoir parameters. In *SPWLA 57th Annual Logging Symposium*. Society of Petrophysicists and Well-Log Analysts.

Gluyas J and Swarbrick R 2013 Petroleum Geoscience. 2nd ed, John Wiley & Sons.

Herrick DC and Kennedy WD 1996 Electrical properties of rocks: effects of secondary porosity, laminations, and thin beds. In *SPWLA 37th Annual Logging Symposium*, Paper C.

Kennedy WD and Herrick DC 2004 Conductivity anisotropy in shale-free sandstone. *Petrophysics* 45(01): 38-58.

Klein JD 1996 Saturation effects on electrical anisotropy. *Log Anal.* 37(01): 47-49.

Klein JD and Martin PR 1997 The petrophysics of electrically anisotropic reservoirs. *Log Anal.* 38(03): 25-36.

Kunz KS and Gianzero S 1958 Some Effects of Formation Anisotropy on Resistivity Measurements in Boreholes. *Geophysics* 23(4): 770-794.

La Vigne J, Herron M and Hertzog R 1994 Density-neutron interpretation in shaly sands. In *SPWLA 35th Annual Logging Symposium*, Paper EEE.

Leveaux J and Poupon A 1971 Evaluation of water saturation in shaly formations. *Log Anal*. 12(04), Paper O.

Lřseth LO, Wiik T, Olsen PA, Becht A and Hansen JO 2013 CSEM exploration in the Barents Sea, Part I-Detecting Skrugard from CSEM. In *75th EAGE Conference & Exhibition incorporating SPE EUROPEC.*

Mollison RA, Schon JS, Fanini ON, Kreigshauser B, Meyer WH and Gupta PK 1999 A model for hydrocarbon saturation determination from an orthogonal tensor relationship in thinly laminated anisotropic reservoirs. In *SPWLA 40th Annual Logging Symposium*, Paper OO.

Moran JH and Gianzero S 1979 Effects of formation anisotropy on resistivity-logging measurements. *Geophysics* 44(7): 1266-1286.

NPD 2019 http://factpages.npd.no/Report (Accessed on 30th March 2019).

Peveraro R 1992 Determination of water resistivity: Part 4. Wireline methods. ME10: Development geology reference manual. *AAPG methods in exploration series*, pp.170-173.

Poupon A, Clavier C, Dumanoir J, Gaymard R and Misk A 1970 Log analysis of sand-shale sequences a systematic approach. *J. Petrol. Technol.* 22(07): 867-881.

Schoen JH, Mollison RA and Georgi DT 1999 Macroscopic electrical anisotropy of laminated reservoirs: a tensor resistivity saturation model. In *SPE Annual Technical Conference and Exhibition*. SPE paper 56509.

Shray F and Borbas T 2001 Evaluation of laminated formations using nuclear magnetic resonance and resistivity anisotropy measurements. In *SPE Eastern Regional Meeting*. SPE paper 72370.

Thomas EC and Stieber SJ 1975 The distribution of shale in sandstones and its effect upon porosity. In *SPWLA 16th Annual Logging Symposium*, Paper T.

Wang H, Barber T, Morriss C, Rosthal RA, Hayden RS and Markley ME 2006 Determining anisotropic formation resistivity at any relative dip using a multiarray triaxial induction tool. *In SPE Annual Technical Conference and Exhibition*, Paper SPE 103113.

Worthington PF 1985 The evolution of shaly-sand concepts in reservoir evaluation. *Log Anal.* 26(1): 23-40.

Worthington PF 2000 Recognition and evaluation of low resistivity pay. *Petroleum Geoscience* 6(1): 77-92.